GEOLOGIE EN MIJNBOUW VOLUME 56(4), p. 363-370 1977

AN EXPERIMENTAL APPROACH TO BASEMENT-CONTROLLED FAULTING

W.T. HORSFIELD[1)]

ABSTRACT

Horsfield, W.T. (1977). An experimental approach to basement-controlled faulting. *In*: R.T.C. Frost & A.J. Dikkers (eds.): Fault tectonics in N.W. Europe. Geol. Mijnbouw, 56, p. 363-370.

To assist in the interpretation of fault structures in the North Sea, a programme of scaled-model experiments was run in a specially-built sandbox. Faults were produced in the sand overburden in response to normal displacement along faults in the underlying basement. Variations in overburden fault geometry were studied in relation to the attitude of basement faults and variations in sand properties. A stereoscopic method was used to analyse successive stages of development.

In the experiments, two stages were observed. Initially, curved precursor faults formed, particularly over high-angle basement faults. These were followed by planar normal faults. Over low-angle basement faults, antithetic as well as synthetic normal faults were prominent.

PURPOSE OF STUDY

Palaeozoic and earlier orogenies are known to have caused considerable faulting and deformation of the basement rocks underlying the North Sea. Major basement faults and lineaments, comparable with those now exposed in Scotland and Scandinavia, can also be expected beneath the post-Carboniferous, oil-bearing North Sea sediments (see Dikkers, this volume). During later tectonic phases these early faults could have controlled the location and geometry of the overburden faults which now define the individual oilfields.

An investigation of the possible geometrical relationships between basement and overburden faulting was therefore considered a useful step towards improved interpretation of specific fault problems. This paper describes some results of scaled experimental studies with a sandbox, in which pre-existing faults in a rigid basement were re-activated to produce faults in the overlying sand. Strike-slip movements were not considered.

Previous sandbox studies reported by Parker & McDowell (1955), Wunderlich (1957) and Sanford (1959) investigated structures produced over vertical basement faults. Numerous additional experiments by Parker were described in company reports, but remained unpublished.

The present study has further investigated inclined basement faults with both steep and gentle dips. In contrast to the earlier experiments, the sand surface was generally kept horizontal by local addition or removal of sand, so as to prevent the development of stresses associated with surface fault escarpments. Improved resolution of the fault-zone development was possible through adoption of a stereophotogrammetric technique.

SCALING CONSIDERATIONS

The use of laboratory models to represent large-scale tectonic phenomena requires careful consideration of scaling rules, as was emphasised by Hubbert (1937). The following discussion is intended to show that, if one considers the sedimentary overburden to have been a moderately cohesive material with frictional plastic behaviour at the time of

1) Koninklijke/Shell Exploratie en Produktie Laboratorium, Volmerlaan 6, Rijswijk, The Netherlands.

faulting, then it can be appropriately modelled in the laboratory using dry sand.

The overburden stress acting on material at depth (l) in the geological *prototype* is:

$$\sigma_p = \rho_p \cdot g_p \cdot l_p$$

and in the *model*:

$$\sigma_m = \rho_m \cdot g_m \cdot l_m$$

where ρ is the density, and g the gravitational acceleration.

Neglecting the very small inertial forces, the ratio between corresponding stress components in model and prototype is then:

$$\frac{\sigma_m}{\sigma_p} = \frac{\rho_m}{\rho_p} \cdot \frac{g_m}{g_p} \cdot \frac{l_m}{l_p}$$

or:

$$\frac{\sigma_m}{\sigma_p} = \frac{l_m}{l_p}$$

since g is the same for both model and prototype, and the density ratio of overburden sediment and sand will be close to unity. Hence, the stresses are scaled by the same ratio as the lengths.

Considering the prototype sediment to show (like sand) a frictional plastic behaviour, provides a further scaling relationship. The principal stresses (σ_1 and σ_3) in both model and prototype, at plastic yielding, have to satisfy Coulomb's yield criterion:

$$(\sigma_1 + \sigma_3) \sin \varphi - (\sigma_1 - \sigma_3) - 2c.\cos \varphi = 0$$

or:

$$c = [(\sigma_1 + \sigma_3) \sin \varphi - (\sigma_1 - \sigma_3)] / 2 \cos \varphi$$

where (c) is the cohesion. Assuming the angle of friction (φ) to be roughly the same in both model and prototype, the cohesion of the model material should be

$$c_m = \left[\frac{\sigma_m}{\sigma_p} (\sigma_1 + \sigma_3)_p \sin \varphi - \frac{\sigma_m}{\sigma_p} (\sigma_1 - \sigma_3)_p\right] \Big/ 2 \cos \varphi =$$

$$= \frac{\sigma_m}{\sigma_p} \cdot c_p$$

Thus:

$$\frac{c_m}{c_p} = \frac{\sigma_m}{\sigma_p} = \frac{l_m}{l_p}$$

Hence, proper scaling requires the cohesive strength to be scaled down by the same factor as stresses and lengths.

To represent a section through the earth's crust some 10 to 100 km in length by a 1 m long model requires a length reduction of 10^{-4} to 10^{-5}. Thus, the cohesion of the prototype material must be reduced in the model by a similar ratio. For a typical value of $\frac{l_m}{l_p} = 5 \cdot 10^{-5}$, a cohesive prototype strength of c_p = 50 bar – which is a realistic value for "soft" sediments – would be scaled down to $2.5 \cdot 10^{-3}$ bar, which corresponds to the weight of about 1.5 cm^3 of sand acting on 1 cm^2. Such a value is so small in comparison with the principal stress values occurring in most parts of the model that the relationship between the yield stresses will be only little affected by using cohesionless sand as model material.

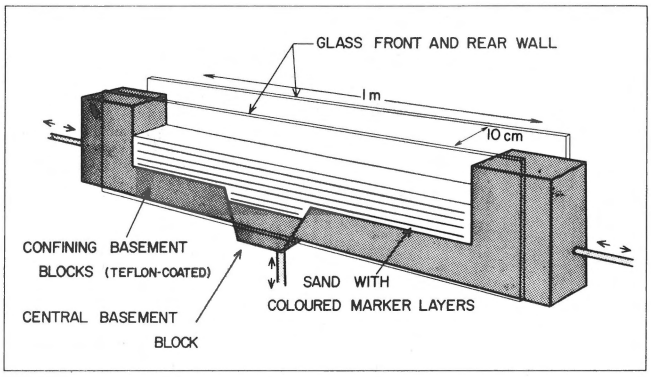

Fig. 1
Sandbox configuration.

Inevitably, scaling is based on idealised models or concepts of material behaviour, and will therefore always exclude some aspects of the real material behaviour. Some doubt must remain about the validity of using sand as a model material without scaling down the grain size in accordance with the length ratio l_m / l_p. Such structural parameters as may be dependent on grain size (e.g. shear zone width) are unlikely to be scaled correctly.

SANDBOX DETAILS

Figure 1 shows the sandbox apparatus constructed for the investigation. A central wedge-shaped basement block, made of teflon-coated PVC, fitted exactly between two confining basement blocks. These latter were free to move laterally on built-in wheels, rolling on the teflon-coated metal base. Wedges of different dip angles (30°, 45°, 60°, 80° and 90°), and of different widths were available. The confining blocks could be moved laterally at a fixed rate of 4.0 mm per minute by a connected motor drive. In this case the central wedge-shaped block was pulled downwards by attached lead weights. Alternatively, the central block could be driven upwards or downwards by another motor, and the confining blocks pulled together by a second set of lead weights. The front and rear panels were made of hardened glass.

Sand was filled into the box by special equipment designed to give a reproducible, homogeneous packing density. It was loaded evenly through a funnel onto a conveyor belt, which then poured the sand through a nest of five trough-shaped sieves (mesh size equivalent to several grain diameters). This method produced uniform sedimentation

across the whole area of the sandbox. The resulting sand pack had an average porosity of 39 – 40% for the grain-size range 0.3 – 0.6 mm diameter. By loading a small amount of ink-stained sand at regular intervals, a series of coloured marker horizons was obtained.

In the course of an experiment the sand surface was kept roughly level by regularly removing uplifted material (using a modified vacuum cleaner) or by filling troughs with extra sand. Photographs were taken at regular intervals.

STEREO COMPARISON

Offsets of marker layers in the sand indicated roughly the position of the faults or shear zones. These were however much more clearly seen afterwards, on comparison of pairs of successive photographs with a pocket stereo viewer. The technique has been described by Butterfield *et al.* (1970). A pseudo-stereo effect is seen because of the incremental displacement of individual sand grains between the two photographs. In the resultant 3-D image, apparent heights represent displacements of sand grains in a direction parallel to a line joining the mid-points of the two photographs. Sharp variations in height (escarpments or cliffs) represent narrow faults or shear zones.

This stereo analysis, which is independent of the use of marker horizons, enables minute incremental displacements between two successive photographs to be studied, rather than the cumulative displacements indicated by the offset of markers. One can therefore define active and extinct shear zones at any given stage. The stereo image may also be contoured to provide detailed maps of the displacement components in any direction. These are of particular value in understanding the manner in which shear zones develop in the sand. A computer program is being developed by R. Harkness of Southampton University to determine strain increments from digitised stereo images.

EXPERIMENTAL RESULTS

A series of experiments was run to study the relation of overburden faulting to the dip of a normal fault in the underlying basement. Using the stereo method to examine the incremental evolution of the structures, it became clear that one could often define two stages of development.

(1) Initial movement was characterised by curved "precursor" faults of minor displacement. These were concave towards the downthrown block and showed movement in the same sense as (i.e. synthetic to) the basement fault.

(2) Subsequently a system of planar normal faults replaced the precursors. These varied in dip between 55° and 90° and included both synthetic and antithetic faults.

The repetition of an experiment did not always give precisely identical results but there were sufficient similarities to enable the following generalisations to be made.

(1) Vertical basement fault

Displacement of the basement along a vertical fault led initially to one or more curved, precursor reverse faults in the overburden above the downthrown block (Fig. 2a). These typically had a very small displacement and, as movement continued, were replaced by steeper reverse faults of lower curvature. Later movement was concentrated on a vertical or steeply-dipping normal fault in the overburden. In the latter case (Fig. 2b), some movement continued also on a steep reverse fault. No antithetic faults formed.

(2) Basement fault dipping at 80°

Curved reverse faults again developed initially (Fig. 2c) but were replaced by a planar normal fault approximately parallel to the basement fault (Fig. 2d). No antithetic faults formed.

(3) Basement fault dipping at 60°

A single curved precursor fault formed (Fig. 3a), of near-vertical attitude. Further movement initiated a steep, synthetic normal fault. In some experiments, this had a dip close to 60°, in others it was somewhat steeper. In the latter case, an antithetic normal fault also developed (Fig. 3b).

(4) Basement fault dipping at 45°

The precursor stage was hardly detectable. A steep normal fault formed first, with a very slight curvature (Fig. 3c). An antithetic fault then developed from the transition point between basement and overburden faults, thus causing a small secondary graben (Fig. 3d). Further synthetic and antithetic faults continued to cause this graben to deepen.

(5) Basement fault dipping at 30°

A steep normal fault, very slightly curved, (Fig. 3e) was followed by planar antithetic and synthetic faults which formed a deep secondary graben (Fig. 3f).

For this particular experimental configuration, the detailed movement of sand grains was studied photogrammetrically. Using selected pairs of photos from different stages of an experiment, the resultant stereo images were plotted as contour maps (Fig. 4). The contours represent incremental displacements between the taking of the two photos. Separate maps were made to show the vertical (y) and horizontal (x) displacements of the sand, respectively.

The maps show (a) the initial broad zone of shear, which then (b) becomes concentrated along a steep, slightly curved path. By this second stage a region of sand has begun to sink with a greater vertical displacement than the basement block. Finally (c) the wide shear zones are seen to have shrunk into a well-defined normal fault and antithetic fault, bounding the secondary graben.

In this experiment no sand was added to maintain a horizontal surface. Some downslope movement of the sand at the free surface fault scarp is suggested by the map (c) of horizontal displacements.

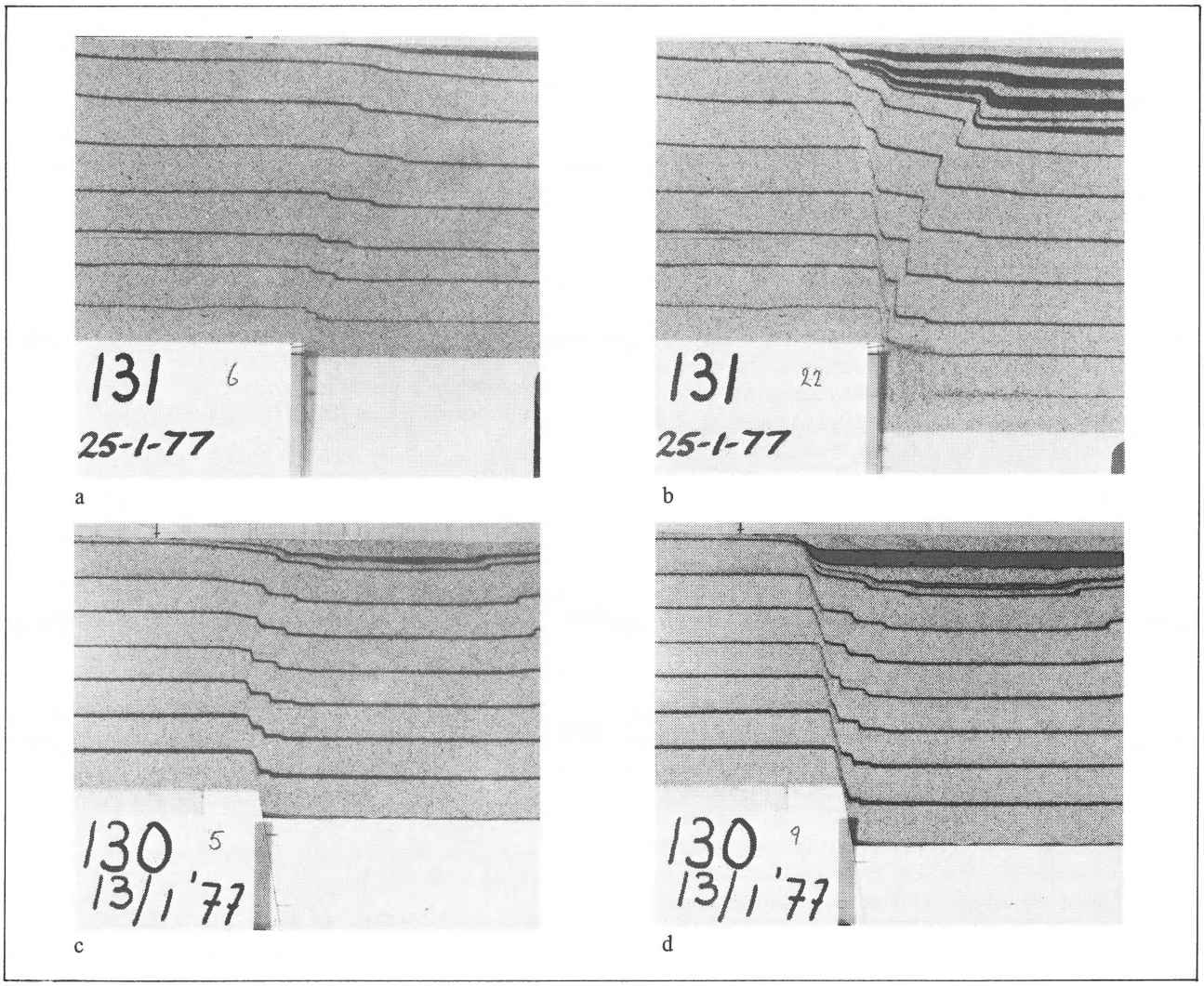

Fig. 2
Development of faults in dry sand overlying steep basement faults, of vertical attitude (photos a, b) and of 80° dip (photos c. d). Left-hand photos are of early stage, showing active precursor faults. Right-hand photos show normal faults formed after further basement movement. Marker horizons of dark sand are at 25 mm vertical spacing. Extra sand was added during displacement to maintain a horizontal free surface.

From the experiments it became clear that (a) precursor faults are most pronounced above high-angle basement faults, and (b) antithetic faults with associated secondary grabens form only when basement faults are less steep than those which tend to form in the overburden. They are most pronounced over low-angle basement faults.

Several experiments were repeated using sand of different grain-size composition, and different packing density. Grain-size variation had little qualitative effect on the structures observed. It was found difficult to achieve a uniform loose sand pack. However, an experiment with a sand pack of porosity nearly 47% suggested that the precursors were suppressed in this loose sand (compare Figs. 5a and 5b).

The frictional influence of the glass sidewalls on movement of the sand has not yet been fully evaluated. In some experiments the fault intersection with the free surface was observed to be slightly bowed, indicating that the sidewalls did restrain sand movement, and that fault dips measured through the glass walls would therefore be a little different from dips in the centre of the sand body. However, this frictional effect is not considered likely to influence the general fault relationships described above.

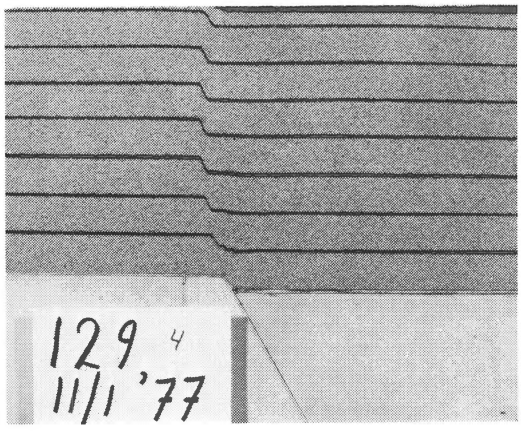

a

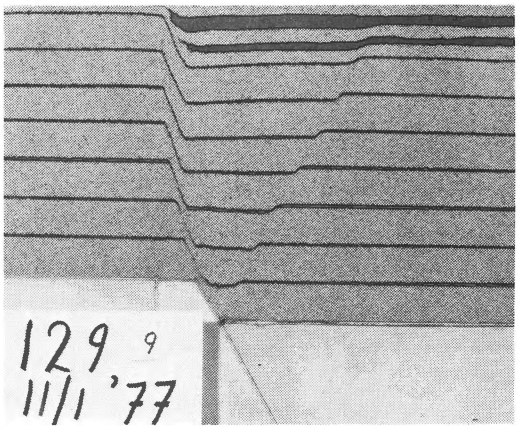

b

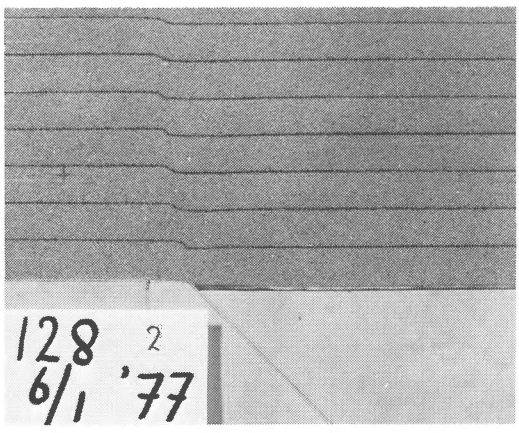

c

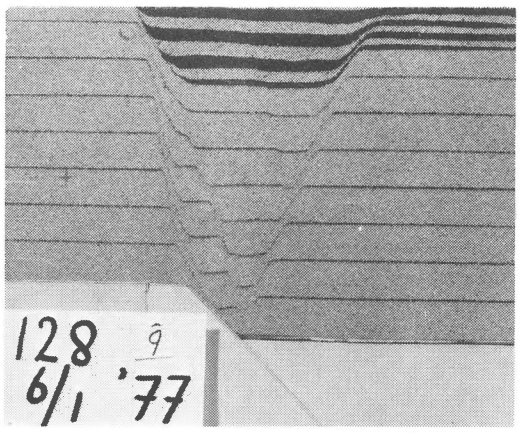

d

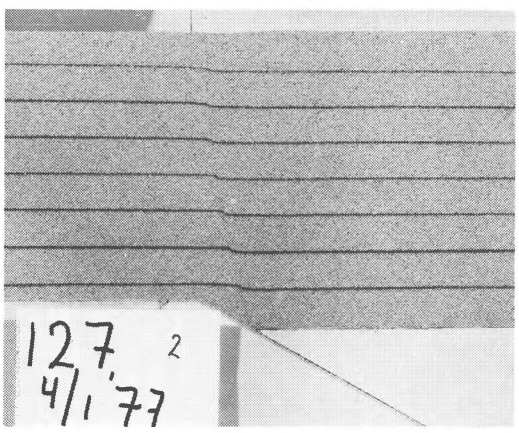

e

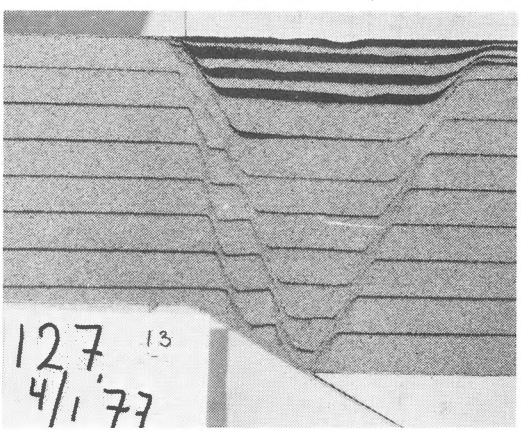

f

Fig. 3
Development of faults in dry sand over low-angle basement faults of dip 60° (photos a, b), 45° (photos c, d) and 30° (photos e, f). Left-hand photos of early stage show precursor faults. Right-hand photos show later secondary graben.

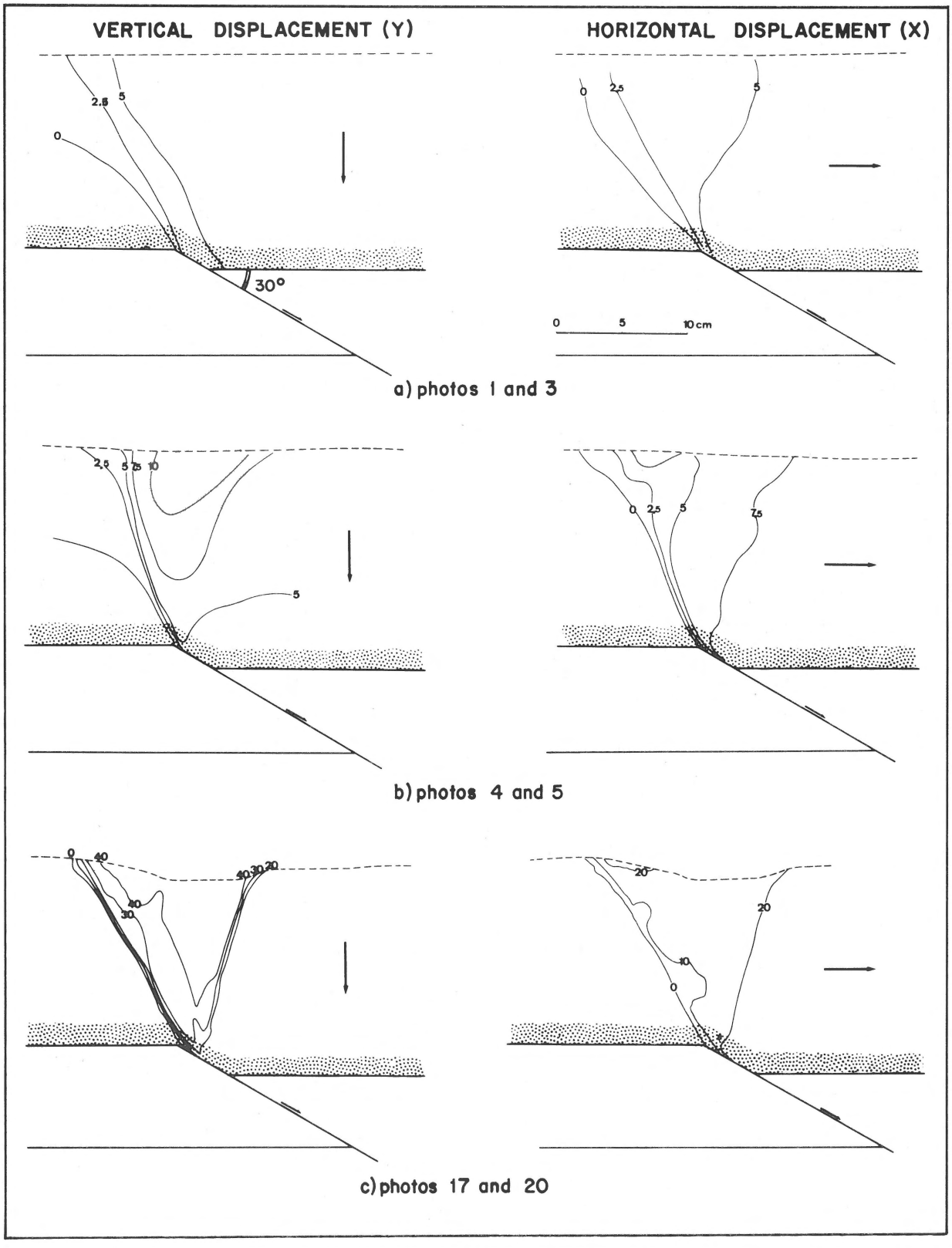

Fig. 4
Displacement maps, drawn from stereo images, of overburden response to movement on a low-angle (30° dip) basement normal fault. Maps at left show component of vertical (y) displacement, maps at right horizontal (x) displacement, for increments at three stages of fault development. Displacements are relative to the left-hand basement block. Contour spacing for (a) and (b) represents 0.25 mm displacement, for (c) 1.0 mm displacement.

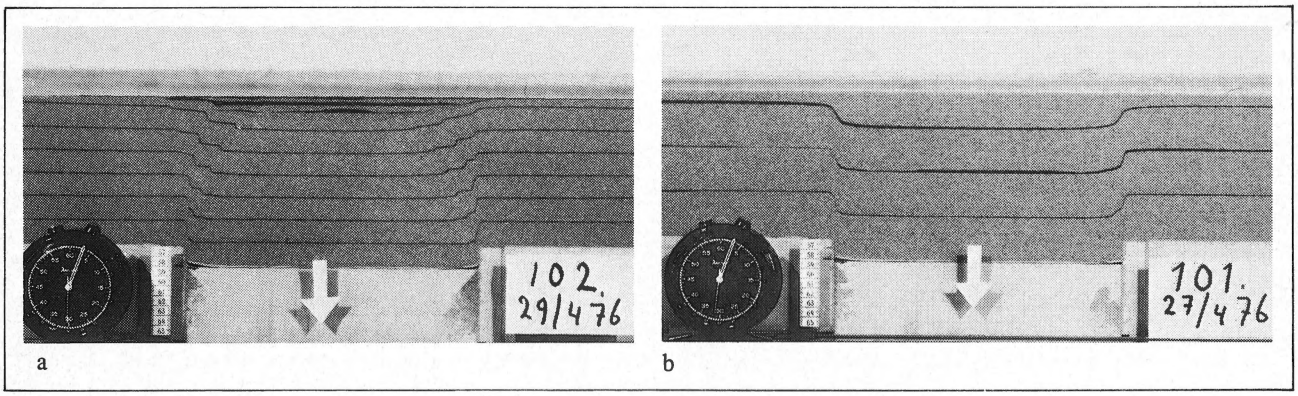

Fig. 5
Comparison of experiments (a) with densely-packed sand of about 40% porosity, and (b) with loosely-packed sand of nearly 47% porosity (grain diameter 0.3 – 0.6 mm in both cases). The central block was displaced downwards by 20 mm. In (a) reverse precursor faults are prominent and the fault zones appear narrower than in (b).

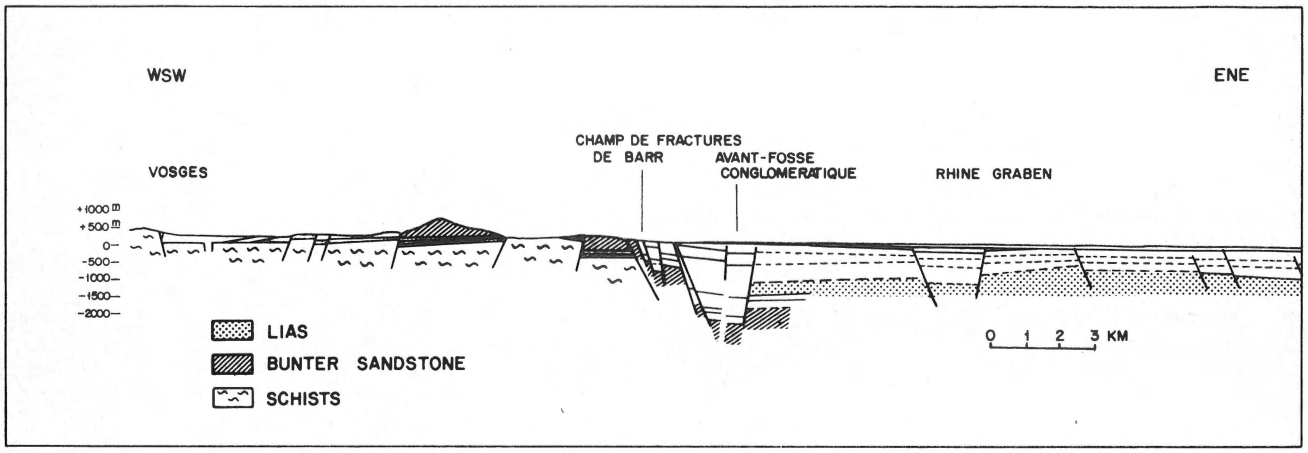

Fig. 6
Section across the western boundary of the Upper Rhine Graben (after Sittler, 1967), showing marginal trough. Compare with Fig. 3.

DISCUSSION

The absence of the distinctive curved precursor faults in a loose sand pack suggests that they are associated with the initial dilatancy of densely-packed sand, when subject to shearing. The dilatancy loosens the sand until a shear zone forms, but it may also disturb the applied stress field so that the orientation of the initial (precursor) shears or faults is controlled by this disturbed state. Subsequently, as shear concentrates along narrow zones, the rate of dilatancy should diminish and the stress field (with its associated shears) can rotate to a more stable attitude.

The amount of dilatancy will relate to the width of the shear zone. As this is not correctly scaled in the sandbox, the extent to which dilatancy and the associated precursors may occur on a geological scale cannot be predicted from our experiments.

The later stages of experimentally-observed faulting are, however, considered truly-scaled replicas of geological fault processes. They can be used in the interpretation of natural examples. The occurrence therefore of antithetic faults and secondary grabens adjacent to a steep normal fault – as has been observed for example in the Rhine Graben (Fig. 6) – would thus suggest continuation at depth into a low-angle fault.

It is intended to compare experimental conclusions with results from a finite-element computer analysis currently being designed at KSEPL.

ACKNOWLEDGEMENTS

F. Lehner designed the sandbox used at KSEPL and initiated the experiments. L. Volkerijk and R.A.J.P. v.d. Akker are thanked for their expert technical assistance, and G. Mandl and other colleagues for many helpful suggestions.

REFERENCES

Butterfield, R., R.M. Harkness & K.Z. Andrawes (1970) – A stereophotogrammetric method for measuring displacement fields Geotechnique, 20, p. 308-314.

Hubbert, M.K. (1937) – Theory of scale models as applied to the study of geological structures. Geol. Soc. Amer., Bull., 48, p. 1459-1520.

Parker, T.J. & A.N. McDowell (1955) – Model studies of salt-dome tectonics. Amer. Assoc. Petrol. Geol., Bull., 39, p. 2384-2470.

Sanford, A.R. (1959) – Analytical and experimental study of simple geological structures. Geol. Soc. Amer., Bull., 70, p. 19-52.

Sittler, C. (1967) – Le soubaissement et le remplissage sédimentaire du fossé rhénan, au niveau du bassin de Pechelbronn et du senil d'Erstein; coupes géologiques à travers le fossé rhénan. *In:* The Rhinegraben progress report 1967, Baden-Württemburg, Geol. Landesamt, Abh., 6, p. 69-80.

Wunderlich, H.G. (1957) – Brüche und Gräben im tektonischen Experiment. N. Jahrbuch Geol. Paläont., Mh., 11, p. 477-498.